

This document is confidential and is proprietary to the American Chemical Society and its authors. Do not copy or disclose without written permission. If you have received this item in error, notify the sender and delete all copies.

Impact of tannin supplementation on proteolysis during post-ruminal digestion in wethers using a dynamic *in vitro* system: a plant (*Medicago sativa*) digestomic approach

Journal:	<i>Journal of Agricultural and Food Chemistry</i>
Manuscript ID	Draft
Manuscript Type:	Article
Date Submitted by the Author:	n/a
Complete List of Authors:	Sayd, Thierry; INRAE Chambon, Christophe; INRAE Popova, Milka; INRAE, UMRH Morgavi, Diego; INRAE, UMRH Torrent, Angelique; INRAE, UMRH Blinet, Sylvie; INRAE Theron, Laetitia; INRAE Niderkorn, Vincent; INRAE, UMR Herbivores

SCHOLARONE™
Manuscripts

1 **Impact of tannin supplementation on proteolysis during post-ruminal digestion in**
2 **wethers using a dynamic *in vitro* system: a plant (*Medicago sativa*) digestomic approach**

3

4 Thierry Sayd¹, Christophe Chambon², Milka Popova³, Diego P. Morgavi³, Angélique
5 Torrent³, Sylvie Blinet¹, Laetitia Theron¹, Vincent Niderkorn^{3,*}

6

7 ¹INRAE, UR 370, Qualité des Produits Animaux (QuaPA), Site de Theix, 63122 Saint-Genès-
8 Champanelle, France

9 ²INRAE, UR 370, Plateforme Exploration du Métabolisme (PFEM) composante protéomique,
10 UR 370, Qualité des Produits Animaux (QuaPA), Site de Theix, 63122 Saint-Genès-
11 Champanelle, France

12 ³Université Clermont Auvergne, INRAE, VetAgro Sup, UMR Herbivores, F-63122 Saint-
13 Genes-Champanelle, France

14

15 *Corresponding author: +33473624069 ; vincent.niderkorn@inrae.fr

16 Abstract

17 The aim of this study was to characterize the effects of tannins on plant protein during sheep
18 digestion, using a digestomic approach combining *in vivo* (rumen) conditions and an *in vitro*
19 digestive system (abomasum and small intestine). Ruminal fluid from wethers infused with a
20 tannin solution or water (control) was introduced into the digester, and protein degradation
21 was followed by LC-MS/MS. Tannin infusion in the rumen led to a clear decrease in protein
22 degradation-related fermentation end-products, whereas RuBisCo protein was more abundant
23 than in control wethers. In the simulated abomasum, peptidomic analysis showed more
24 degradation products of RuBisCo in the presence of tannins. The effect of RuBisCo protection
25 by tannins continued to impact Rubisco digestion into early-stage intestinal digestion, but was
26 no longer detectable in late-stage intestinal digestion. The peptidomics approach proved a
27 potent tool for identifying and quantifying the type of protein hydrolyzed throughout the
28 gastrointestinal tract.

29

30 *Keywords:* protein, tannins, *in vitro* digestion, rumen, abomasum, intestine, proteomics,
31 peptidomics, ruminant

32 1. Introduction

33 The world's population is projected to increase from 7.9 billion people in 2021 to 9.7 billion
34 by 2050¹, bringing a 50% increase in global demand for food protein driven largely by rising
35 incomes in developing countries.² The production of protein for human consumption carries
36 economic, social and environmental dimensions that need to be integrated at all levels of the
37 food chain in order to find a sustainable balance.³ Ruminant-based protein is heavily
38 challenged as a viable source, as transfers of dietary nitrogen (N) into milk and meat are
39 known to be inefficient (around just 25%) in ruminants.⁴ This low N utilization by ruminants
40 is mainly due to excessive degradation of dietary protein in the rumen causing unavoidable N
41 losses in urine that create an environmental burden through ammonia (NH₃) volatilization and
42 nitrate leaching. Furthermore, microbial nitrification and denitrification processes partly
43 transform urinary N in the soil into nitrous oxide (N₂O), which is a greenhouse gas (GHG)
44 that has a global warming potential 300 times greater than CO₂.^{5,6} Compounding this issue,
45 ruminants in some production systems consume high amounts of soybean meal, which is
46 mainly imported from South-America and known to be responsible for land-use change and
47 concomitant GHG emissions.⁷ The efficiency of N utilization by ruminants can be improved
48 by optimizing the supply of rumen-degradable protein to decrease N losses, and by improving
49 the efficiency of utilization of absorbed amino acids.^{8,9}

50 In ruminants, N flow to the small intestine is in the form of rumen microbial protein and
51 dietary protein that is not or only partly degraded in the rumen.¹⁰ The protein reaching the
52 intestine are degraded in aminoacids which can be absorbed by the animal. One option to
53 increase the rumen bypass protein is to use tannins that can complex proteins and partly
54 protect them against rumen degradation.¹¹ However, the effect of tannins on the fate of
55 proteins as they transit through the whole gastrointestinal tract remains largely unknown. In
56 particular, the series of different digestive compartments exposes ingested protein to a series

57 of changing pH and enzymatic conditions that are liable to lead to drastic changes in protein
58 degradation.

59 To address this gap, this study set out to characterize the effects of a tannin extract on the
60 digestion of dietary protein in the rumen and in conditions simulating the post-rumen
61 digestive compartments, i.e. the abomasum and the small intestine, using an original dynamic
62 *in vitro* system coupled with a digestomic approach using high-resolution mass spectrometry.

63

64 **2. Materials and methods**

65 The experiment was conducted at the INRAE Clermont Auvergne Rhône-Alpes center in
66 Theix, France. All animal-related experimental procedures were conducted in accordance
67 with the EU Directive 2010/63/EU, reviewed by the local institutional animal care and use
68 comitee (C2E2A, “Comité d’Ethique pour l’Expérimentation Animale en Auvergne”), and
69 pre-authorized by the French Ministry for Research (approval # 7138-2016092709177605-
70 V5).

71

72 ***2.1 Animal feeding and treatments***

73 The study used six Texel wethers (age = 6.5 ± 1 years, weight = 75.9 ± 5.9 kg, body condition
74 score = 2.5 ± 0.3) equipped with rumen cannula. The wethers were fed for one week on 1.5
75 kg/day of alfalfa (*Medicago sativa*) hay (chemical composition, in g/kg dry matter: organic
76 matter (OM) = 903, crude protein (CP) = 135, neutral detergent fibre (NDF) = 484, acid
77 detergent fibre (ADF) = 345) in two equal meals at 8 a.m. and 4 p.m., and had free access to
78 water and salt blocks. The wethers were then randomly separated into two equal groups that
79 were treated or not with tannins for two more weeks. Wethers were fed as in the previous
80 week and every day before afternoon feeding, sheep from one group (tannin group) were
81 infused through the rumen cannula with 500 mL of an aqueous solution containing 100 g of

82 an extract of quebracho and chestnut tree tannins (Silvafeed® ByPro, Silvateam, San Michele
83 Mondovi, Italy), while sheep from the other group (control group) were infused with water.
84 The solutions were infused in four 125-mL doses at 5-min intervals, using a 200-mL syringe.
85 Throughout the experiment, wethers had no health issues and consumed all offered daily
86 amounts of alfalfa.

87

88 ***2.2 Sampling and preparation of rumen fluid***

89 After three weeks, rumen contents were withdrawn from the reticulum before the morning
90 feeding and immediately squeezed through a polyester monofilament fabric (mesh size: 800
91 μm) to obtain rumen fluid with a standardized particle size. The filtered rumen fluid was kept
92 in a tightly-closed Thermos flask until transfer to the laboratory. Time from rumen content
93 withdrawing until introduction in the digester did not exceed 30 min. An aliquot of rumen
94 fluid (5 mL) was transferred into a polypropylene tube containing 0.5 mL of H_3PO_4 5% (v/v)
95 and frozen at -20°C for NH_3 analysis. A second aliquot (0.8 mL) was transferred into a
96 microtube containing 0.5 mL of deproteinizing solution (crotonic acid 0.4% w/v and
97 metaphosphoric acid 2% w/v in HCl 0.5 M), and the mixture was cooled at 4°C for 2 h,
98 centrifuged at 16,500 g for 10 min at 4°C , and the supernatant was frozen at -20°C for
99 volatile fatty acids (VFA) analysis. Four 25-mL Falcon® tubes of rumen fluid were also taken
100 and immediately stored at -80°C for proteomic and microbial analysis.

101

102 ***2.3 Rumen proteomic analysis***

103 Proteins were extracted from strained rumen samples, obtained as described in section 2.2.
104 First, samples were centrifuged at 10,000 g for 30 min at 4°C . Then, the supernatant was
105 homogenized in 15% trichloroacetic acid (TCA) and centrifuged at 14,000 g for 30 min at
106 4°C . The supernatant was discarded and precipitate was homogenized for 30 min in 62.5 mM

107 Tris (pH 6.8), 2% SDS and 5% 2-mercaptoethanol using a MM2 glass bead agitator (Retsch,
108 Haan, Germany). The homogenate was centrifuged at 10,000 g for 15 min at 4°C. The pellet
109 was discarded and the supernatant was frozen at -80°C until further analysis.
110 The samples were prepared for proteomic analysis.¹² Briefly, samples were heated at 95°C for
111 5 minutes and loaded onto SDS-PAGE (12% acrylamide) to concentrate the proteins. The gel
112 was stained using Coomassie Blue G-250, and the bands were excised, reduced in 10 mM
113 dithiothreitol in 50 mM ammonium bicarbonate, and alkylated in 55 mM iodoacetamide in 50
114 mM ammonium bicarbonate.
115 The strips were then destained with a 50% acetonitrile solution containing 25mM ammonium
116 bicarbonate, dehydrated with a 100% acetonitrile solution and dried by 5 min at speed Vac.
117 Protein hydrolysis was performed with 30 µL of a trypsin solution (10 ng/µL in 25mM
118 ammonium bicarbonate; V5111, Promega) overnight at 37°C. Peptides were extracted with 50
119 µL of an acetonitrile/formic acid solution, 99.9/0.1 under ultrasound (15 min). The
120 hydrolysates were then dried and recovered in 20 µL of 0.1% formic acid solution for LC-
121 MS/MS analysis.

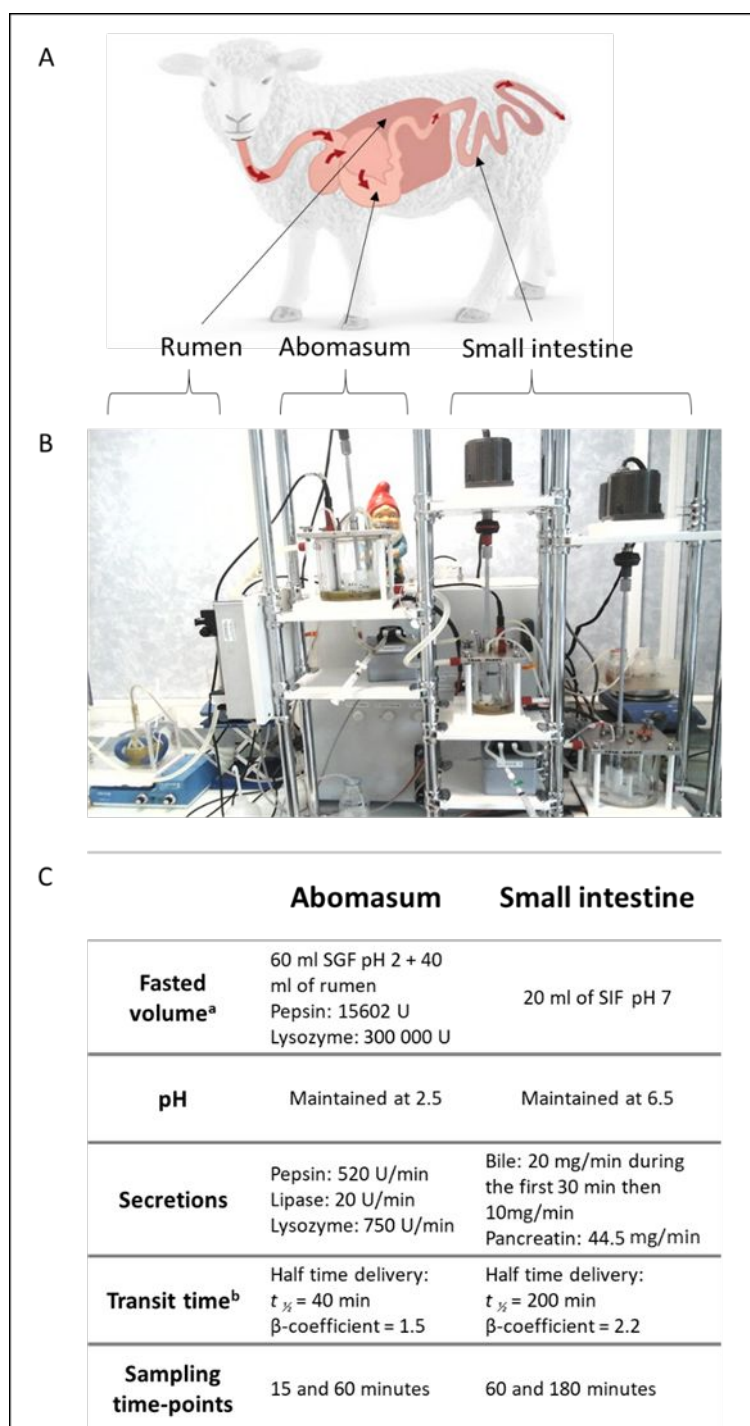
122

123 ***2.4 In vitro dynamic abomasal–intestinal digestion***

124 Post-rumen digestion was performed using an *in vitro* dynamic system (DIDGI®; INRAE,
125 Paris, France).¹³ Briefly, the system was composed of an abomasal compartment followed by
126 two consecutive intestinal compartments: the duodenal–jejunal compartment and the intestinal
127 compartment (Figure 1A-B). Each compartment emptied into the next one using a calibrated
128 peristaltic pump. The regulation of pH and temperature was controlled by electrode probes in
129 the abomasal and duodenal–jejunal compartment. pH in these two compartments was
130 dynamically adjusted by two pumps adding HCl and NaHCO₃, respectively. The rumen fluid

131 and abomasal digestive enzyme mixtures were added by peristaltic pumps. The whole system
132 was managed using StoRM® software.¹⁴
133 The parameters used in the *in vitro* abomasal–intestinal digestion study are summarized in
134 Figure 1C.^{15,16} To mimic the abomasal compartment, the initial mix used 60 mL of simulated
135 abomasal fluid with 15,600U of pepsin and 300,000U of lysozyme, and 40 mL of ruminal
136 fluid. pH was adjusted to 2.5 with HCl. The flux of rumen fluid entering the abomasal
137 compartment was set at 2.5 mL/min during 60 min. Four pumps were used to automatically
138 regulate pH at 2.5 with HCl and to infuse an enzyme mix (pepsin, 520 U/min; lipase:
139 20U/min; lysozyme, 750 U/min) into the compartment. The rumen fluid was added at a
140 flowrate of 2.5 mL/min for 60 min. To mimic the intestinal digestion, the compartment was
141 filled with 20 mL of simulated intestinal fluid. During digestion assay, the bile was added at
142 20 mg/min during the first 30 min, and then 10 mg/min. The pancreatin was added at 44.5
143 mg/min. The abomasal and intestinal emptying rates followed the equation $f = 2^{-(t/t_{1/2})\beta}$.¹⁶
144 Emptying half-times were 40 min and 200 min for the abomasal and intestinal compartments,
145 respectively, and pH was kept at a constant 2.5 and 6.5, respectively.

146



147

148 **Figure 1.**

149

150 The digests were sampled at 15 and 60 min in the abomasal compartment (named A15 and

151 A60) and at 60 and 180 min in the intestinal compartment (named I60 and I180). The

152 collected digests were filtered through gauze swabs, and the filtrate was put on ice. The

153 proteins were precipitated with cold TCA (15% final concentration) for 1 h, then the tubes

154 were centrifuged at 4,000 g for 15 min at 4°C. The supernatant, containing the peptides
155 resulting from digestion, was kept at -20 °C until further analysis.

156

157 ***2.5 Rumen fermentation end-products and microbial analyses***

158 The VFA profile (acetate, propionate, butyrate, valerate, isobutyrate and isovalerate) in rumen
159 fluid was determined by gas chromatography using crotonic acid as internal standard on a
160 Perkin Elmer Clarus 580 GC (Perkin Elmer, Courtaboeuf, France).¹⁷ For the NH₃
161 concentration in rumen fluid, samples were centrifuged at 10,000 g for 10 min, and NH₃ was
162 determined in the supernatant using the Berthelot reaction.¹⁸ The reaction was carried out in
163 duplicate in 96-well plates using an Infinity M200 spectrophotometer (Tecan Austria GmbH,
164 Grödig, Austria).

165 For microbial analyses, frozen rumen fluid samples were ground to a fine powder using a
166 chilled grinder (IKA A11 Analytical mill, Staufen, Germany) and liquid N. Genomic DNA
167 was then extracted from approximately 250 mg of sample.¹⁹ Total genomic DNA was sent to
168 the ADNid Laboratory (Qualtech Groupe, France) for Illumina sequencing using primers
169 targeting bacterial 16S rRNA (V3-V5 region) and 18S rRNA genes for protozoa.²⁰

170

171 ***2.6. Digest peptidomic analysis***

172 The following peptide extraction was conducted on the digest extracts precipitated by TCA
173 (see section 2.4).²¹ Briefly, peptide extraction was performed using 25 mg of MCM-41 porous
174 silica nanoparticles (Sigma Aldrich) hydrated with 1 mL of 3% TCA. The resulting slurry was
175 processed ultrasonically, then 300 µL of the TCA sample was added immediately and shaken
176 for two hours at 4°C. The suspension was centrifuged at 4000 g for 15 minutes, and the
177 supernatant was removed. The silica nanoparticles were then washed 3 times with 1 mL H₂O.
178 The peptides retained on the porous silica nanoparticles were eluted with 1 mL of 80%

179 acetonitrile. Extracts were dried in a SpeedVac vacuum concentrator and solubilized with a
180 H₂O/trifluoroacetic acid (100/0.05) buffer. The samples were kept at -20°C until LC-MS/MS
181 analysis.

182

183 ***2.7. Peptide and protein identification and quantification by nano-LC-MS/MS analysis***

184 Briefly, samples from gel-immobilized protein band hydrolysates (see section 2.3) and
185 peptides from the digestion of ruminal, abomasum or intestinal contents (see section 2.6) were
186 injected into a nano-LC-MS/MS system for analysis. The nano-LC-MS/MS system used was
187 a high-resolution mass spectrometer (Thermo-Fisher Scientific, Villebon-sur-Yvette, France),
188 LTQ Velos Orbitrap for abomasal and intestinal samples or a HFX Orbitrap for rumen
189 samples. The volume injected was 1 µL for proteomics and 3 µL for peptidomics. The
190 separation by liquid chromatography was performed on an Ultimate 3000-model nano-HPLC
191 system (Thermo-Fisher Scientific, Villebon-sur-Yvette, France) with a desalting and
192 concentration step on a loading column (300 µm, 0.5 cm, Thermo-Fisher Scientific, Villebon-
193 sur-Yvette, France). The peptides were separated on a 75-µm, 15 cm Accucore or 25 cm
194 Acclaim C18 column (Thermo-Fisher Scientific, Villebon sur Yvette, France) using an
195 acetonitrile gradient from 4% to 35% during 60 minutes. The peptides were then
196 nanoelectrosprayed into the source and analyzed in data-dependent top-10 mode (LTQ Velos
197 Orbitrap, Thermo-Fisher Scientific, Villebon-sur-Yvette) or top-18 mode (HFX Orbitrap,
198 Thermo-Fisher Scientific, Villebon-sur-Yvette).

199 Next, raw files were loaded and processed for quantification analysis using Progenesis QI
200 (Nonlinear Dynamics, Waters, Newcastle, UK) software.²¹ The LC-MS runs were
201 automatically aligned prior to ion detection and normalization. For peptide and protein
202 identification, the list of MS/MS spectra of all the peaks detected was exported from the
203 Progenesis QI software to MASCOT (v2.5) or Peaks (vX+) in file format (.mgf). The

204 database used was ‘Medicago_sativa’ extracted from NCBI (2020,1099 sequences). The
205 search parameters were set as follows: no enzyme for peptidomic (abomasal–intestinal
206 digestion) analyses, trypsin for proteomic (rumen) analyses, MS mass tolerance at 15 ppm for
207 peptides and 0.02 Da for fragments, with a possible mass adduct of methionine oxidation.
208 Peptide identification was validated when ions had a significant Mascot score at a false-
209 positive rate of < 0.05. The identification results were then re-imported into Progenesis IQ for
210 peptide quantification. For protein quantification, only peptides with a sequence shared by a
211 single protein were used to compute normalized abundance. We therefore summed these
212 abundances of each peptide for a protein to give the normalized abundance of the protein in
213 the sample. This abundance value of the protein was then used to assess the intensity of
214 protein hydrolysis during digestion.

215

216 ***2.8 Bioinformatics and statistical analysis***

217 Data on rumen fermentation end-products (VFA and NH₃) were analyzed with R (v3.5.1)
218 using a mixed linear model that included tannin infusion as fixed effect and animal donor of
219 rumen fluid as random effect.

220 Principal component analysis (PCA) was run on tannin and control samples at the different
221 incubation points after 15 (A15) and 60 (A60) min of digestion in the abomasum, and
222 confidence ellipses were calculated using R. Statistical terms enrichment analysis was
223 performed using the Panther tool (<http://pantherdb.org>)²² and Gene Ontology (GO) cellular
224 compartment information, and the results were represented at cellular level using
225 Compartment, a web localization tool (<http://compartments.jensenlab.org>).²³ Peptigram was
226 used to visualize and graph the peptides released during abomasal and intestinal digestion of
227 large-chain and photosystem-I RuBisCo proteins along the protein sequence
228 (<http://bioware.ucd.ie/peptigram>).²⁴

229 The DNA sequences were analyzed using the FROGS computational pipeline.²⁵ On average,
230 per sample and after trimming read quality, we obtained 50005 (± 13426) reads for bacterial
231 16S rRNA genes and 15693 (± 8575) reads for eukaryotic 18S rRNA genes. Operational
232 taxonomic unit (OTU) tables were analyzed in R using the ‘vegan’ package.²⁶ Diversity
233 indices (Shannon, Simpson, Richness and Evenness) were computed using implemented
234 functions, and statistical differences were tested using the non-parametric Kruskal-Wallis test
235 to evaluate the plant effect at each incubation time. For β -diversity analysis, OTU tables were
236 rarefied to an even depth, giving 33389 reads for bacteria and 1200 for protozoa. Dissimilarity
237 indices were computed by the Bray-Curtis method using the vegdist function. PCA was
238 performed on the dissimilarity matrices using the rda function. Permutational multivariate
239 analysis of variance was performed using the Adonis function after first checking the
240 variability of dispersion (betadisper function). Indicator OTUs were identified using the
241 multipatt function of the R package ‘indicspecies’.

242

243 **3. Results**

244 ***3.1. Rumen fermentation end-products***

245 Total VFA concentration in the rumen was 10% lower for wethers infused with the tannin
246 extract than for controls (Table 1, $p < 0.001$). The tannin group had lower concentration of
247 acetate (-11%, $p < 0.001$) and tended to have lower propionate concentrations (-7%, $p =$
248 0.061) and a higher acetate:propionate ratio (+13%, $p = 0.070$) than the control group. The
249 tannin group had also lower concentrations of metabolites markers of protein degradation,
250 NH_3 (-28%), isobutyrate (-37%) and isovalerate (-24%) compared to controls ($p < 0.001$).

251

252 ***3.2. Rumen bacterial and protozoal communities***

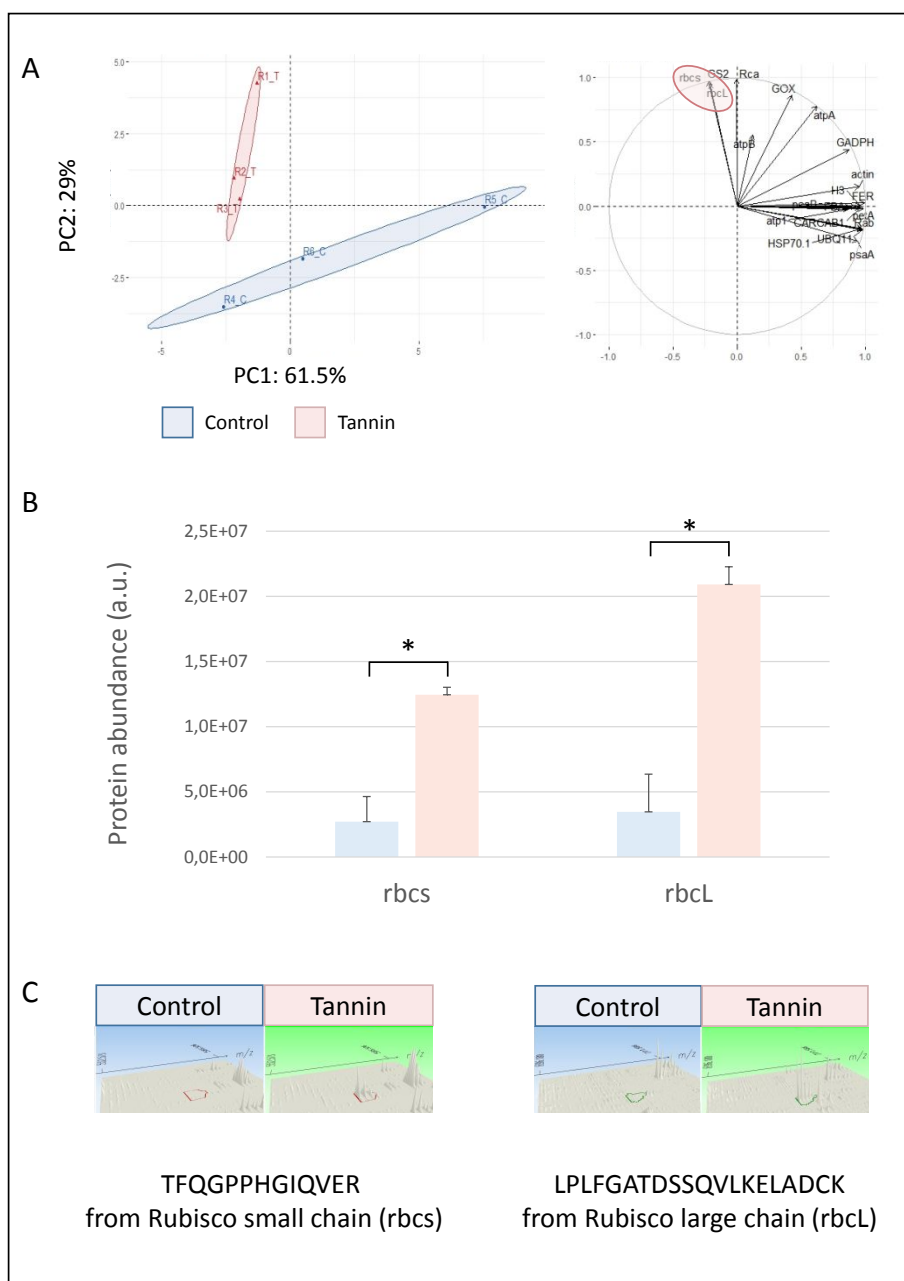
253 Bacterial diversity in the rumen was lower in the tannin group than the control group, as
254 shown by the significant decreases in Shannon, Simpson, Evenness, and Richness indices ($p =$
255 0.049, Figure S1). Adonis tests revealed that community structure differed between the tannin
256 and control as shown in the PCA graph (Figure S2). A total of 181 indicator OTUs were
257 identified for the control group, and 19 indicator species were identified for the tannin group.
258 In total, 79 out of 181 indicator OTUs (44%) identified for the control group were affiliated to
259 the Firmicutes. They were essentially members of the Clostridiales order with
260 Ruminococcaceae representing 20%. In contrast to bacteria, protozoal diversity was
261 unaffected by tannins, except for Richness index which increased in the tannin group (Figure
262 S3). Five protozoal indicator species were identified for the tannin group. Adonis tests and
263 PCA found that protozoal community structure tended to differ between control and tannin
264 groups (Figure S4).

265

266 ***3.3. Proteomic analysis of forage digestion in rumen fluids***

267 The proteomic analysis based on 140 unique peptides identified 20 *Medicago* proteins with at
268 least two unique peptides (see supplementary information, Table 1a of Chambon et al., 2021).
269 Among these proteins, five showed differences intensities ($p < 0.05$) (see supplementary
270 information, Table 1b of Chambon et al., 2021). Three soluble proteins (HSP70-1, Rab and
271 UBI1) showed higher intensities in control rumen fluid ($p < 0.05$), whereas two soluble
272 proteins showed higher intensities in the tannin-group rumen fluid ($p < 0.05$). These two
273 proteins were ribulose biphosphate carboxylase (RuBisCo) small-chain (rbcS) and ribulose
274 biphosphate carboxylase large-chain (rbcL). These differences in protein intensities explained
275 the separation of the two groups on the PCA (Figure 2A). The projection on the first two
276 dimensions (61% and 29% of variance explained by dimensions 1 and 2, respectively) clearly
277 differentiates the rumen fluid of tannin-group wethers from controls. In particular, RuBisCo

278 showed higher abundances in tannin-group rumen than control rumen (Figure 2B), as
 279 represented by the 3D profile of the peptides with the highest intensity identified in rbcs
 280 (TFQGPPIHIQVER) and rbcl (LPLFGATDSSQVLKELADCK) chains (Figure 2C).
 281



282
 283 **Figure 2.**

284

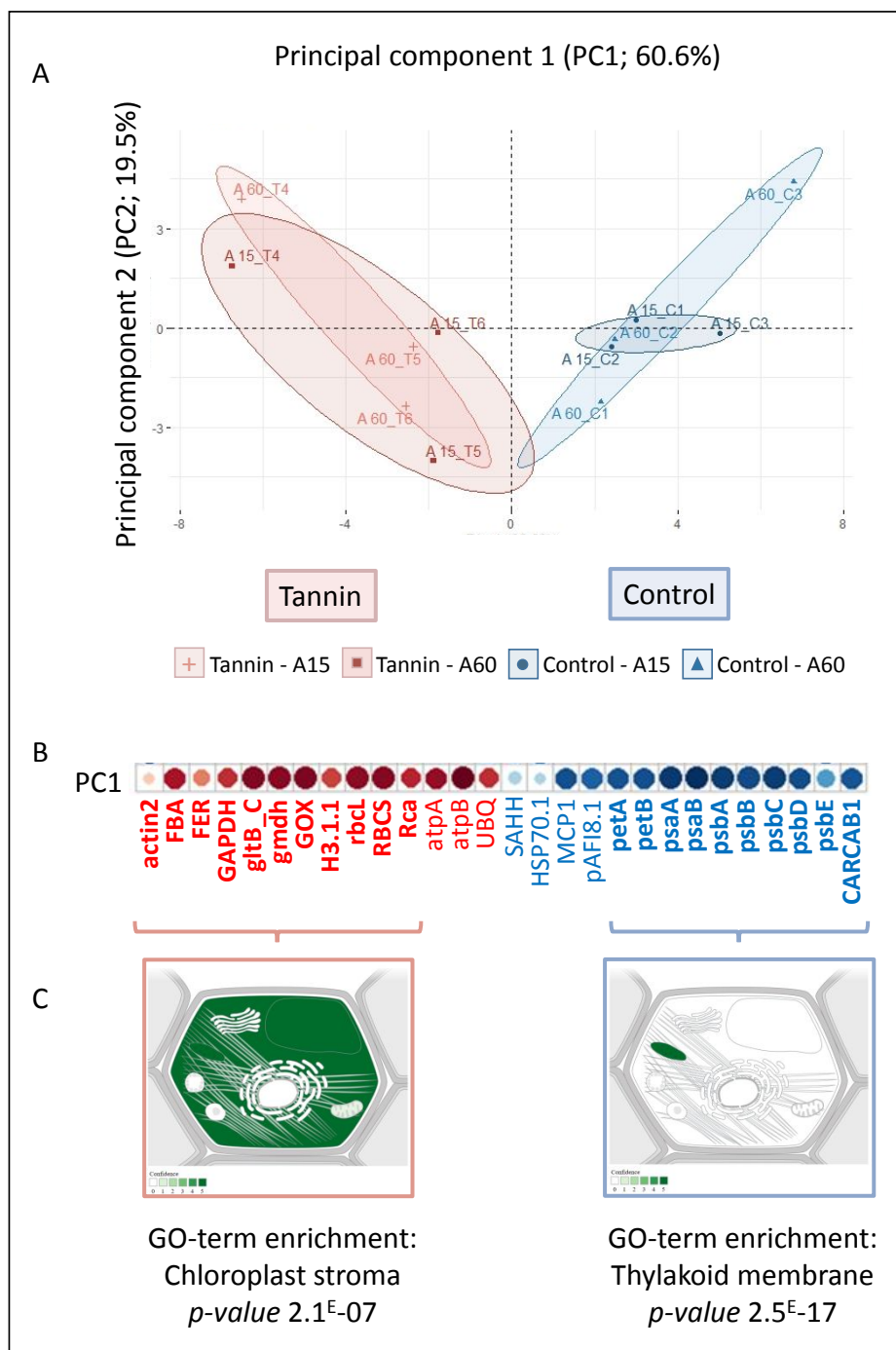
285 **3.4. Peptidomic analysis of the in vitro digestion of forage protein in the abomasum**

286 The peptidomic analysis of the simulated abomasum digestion based on 363 unique peptides
287 identified 28 *Medicago* proteins with at least two unique peptides (see supplementary
288 information, Table 2a of Chambon et al., 2021). Unique peptide abundances were summed for
289 each protein and used to assess intensity of protein hydrolysis based on the principle of
290 peptide release during digestion. Differential intensities were found for 19 proteins ($p < 0.05$)
291 (see supplementary information, Tables 2b and 2c of Chambon et al., 2021): 8 membrane
292 proteins showed higher intensities in the tannin group, with fold changes ranging from 2 to 9,
293 and 11 soluble proteins showed higher intensities in the control group. These differences lead
294 to a clear distinction in the PCA (Figure 3A). The score plot separated the ‘Tannin’ (in red)
295 and ‘Control’ (in blue) samples along the first dimension with 60.6% of variance explained by
296 PC1 and 19.6% by PC2. This distinction was observed regardless the incubation points.
297 Indeed, digests sampled after 15 and 60 minutes of abomasal digestion (A15 and A60,
298 respectively) were not discriminated.

299 The protein hydrolysis profiles between simulated *in vitro* digestion in abomasum of tannin-
300 group and control wethers differed in terms of the protein targets, as illustrated in their
301 contribution to PC1 on the loading plot (Figure 3B). The left part plots the proteins found to
302 be more intense in the abomasal compartment in tannin-group samples. The Gene Ontology
303 term enrichment analysis showed a statistical occurrence of the ‘chloroplast stroma’ cellular
304 compartment (p -value 2.1^E-07) (Figure 3C). The associated proteins were metabolism
305 proteins, such as RuBisCo chain proteins (RCA, rbcL and RBCS genes), and ATPase (atpA
306 and atpB genes), a membrane protein with a stroma structure. The right part plots the proteins
307 found to be more intense in the abomasal compartment in control samples. The Gene
308 Ontology term enrichment analysis revealed a statistical occurrence of thylakoid membrane
309 proteins (p -value 2.5^E-17) (Figure 3C), which belong to photosystems I (psaA and psaB

310 genes) and II (psbA, psbB, psbC, and psbD genes), cytochrome proteins (psbE, petA, and
 311 petB genes), and transmembrane aquaporin-like protein (pAFI 8-1 gene).

312



313

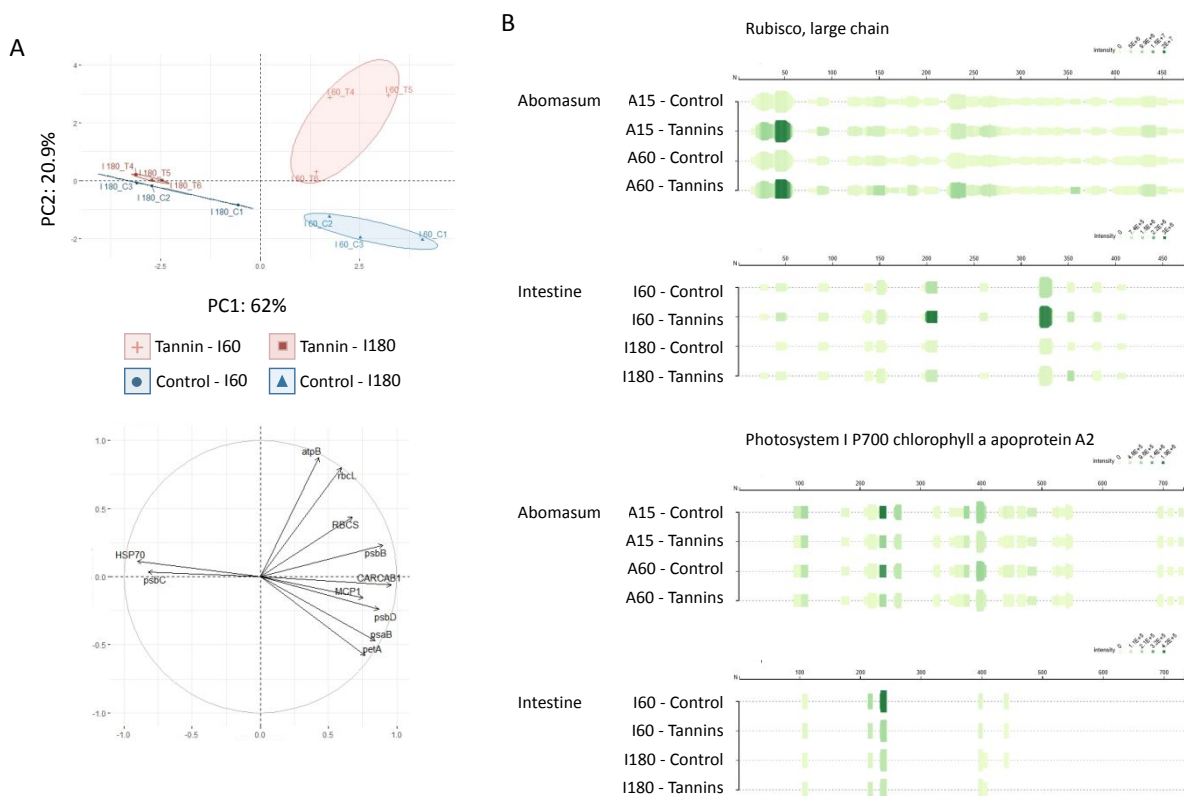
314 **Figure 3.**

315

316 **3.5. Peptidomic analysis of the *in vitro* digestion of forage protein in the small intestine**

317 The peptidomic analysis of the simulated small intestine digestion based on 63 unique
318 peptides identified 11 *Medicago* proteins (see supplementary information, Tables 3abc of
319 Chambon et al., 2021). Despite the substantial decrease in identification translating the
320 digestion of peptides and proteins, the PCA separated tannin-group and control wethers along
321 the first dimension with 62% of variance explained by the PC1 and 20.9% by PC2 (Figure
322 4A). The PCA also showed a different projection according to incubation points, with a clear
323 separation at the earlier stage of intestinal digestion after 60 min (I60). After 60 min of
324 intestinal digestion, the separation was mainly explained by PC2, which is supported by the
325 RuBisCo abundance. The peptides from RuBisCo digestion were more abundant in the
326 intestine in tannin-group samples. At the final stage of intestinal digestion after 180 min
327 (I180), there was no longer a distinction between the peptidomic profile of digestion with vs
328 without tannin infusion. The projection of identified peptides along the protein sequence
329 confirmed this observation, as shown for one protein representative of the soluble fraction, i.e.
330 RuBisCo large chain (*rbcL* gene), and one photosystem-I protein representative of the
331 membrane fraction (*psaB* gene) (Figure 4B).

332



333

334 **Figure 4.**

335

336 **4. Discussion**

337 The main objective of this study was to investigate the effect of tannins on the fate of dietary
 338 protein throughout the ruminant digestive tract using a dynamic *in vitro* digester in controlled
 339 conditions. The dose of tannin extract was chosen to be high without being toxic.²⁷ As
 340 expected, infusion of the tannin extract in the rumen led to a clear decrease in ruminal protein
 341 degradation, as evidenced through the large decrease in isobutyrate and isovalerate
 342 concentrations in the rumen fluid. These two VFAs are branched-chain molecules derived
 343 exclusively from oxidative deamination of branched-chain aminoacids (valine, isoleucine, and
 344 leucine), which makes them relevant as indicators of the extent of protein degradation.²⁸ The
 345 reduction of ruminal proteolysis in the presence of tannins was also confirmed by the large
 346 decrease in ruminal NH_3 concentration resulting from aminoacid deamination, although NH_3
 347 has to be considered as a pool of various fluxes (production from degradation of nitrogenous

348 compounds, absorption across the rumen epithelium, and consumption for urea and microbial
349 protein synthesis).²⁹ In comparison, the decrease in major VFA concentrations in the tannin-
350 group rumen was much smaller (acetate and propionate) or not significant (butyrate). Given
351 that these VFA are fermentation end-products from the degradation of both dietary
352 carbohydrates (cellulose, hemicelluloses and sugars) and proteins³⁰, our results show that
353 tannins primarily affected protein catabolism rather than carbohydrate catabolism. However,
354 the trend towards a between-group difference in acetate:propionate ratio suggests that tannins
355 may have affected the microbiota and its activity. Tannins bind protein but they can also bind
356 to fibres and interact with rumen microbes.³¹ Here, despite the small number of experimental
357 animals, we found a decrease in bacterial diversity and changes in bacterial taxonomy in the
358 rumen from tannin-infused wethers. Bacteria affiliated to the Firmicutes, especially members
359 of the Clostridiales order (mainly Ruminococcaceae), were a discriminant feature of the
360 control group, suggesting that tannins may have affected their distribution. Using a similar
361 tannin extract, a higher proportion of the Firmicutes phyla was reported in dairy cows³²,
362 suggesting an effect of animal type on rumen microbial ecosystem response to tannins.
363 The proteomic analysis aimed to identify proteins in rumen fluids and determine whether
364 tannins affected their abundances. Analysis of rumen fluid showed a higher protein abundance
365 in tannin-group rumen, which confirms the protective effect of tannins against excessive
366 ruminal degradation. Interestingly, PCA analysis showed that separation of the tannin and
367 control groups was mainly due to differences in the abundance of both large and small
368 subunits of RuBisCo (tannin group > control group). RuBisCo, which is the key enzyme
369 responsible for photosynthetic carbon assimilation, emerges as a particularly relevant protein
370 model to investigate the plant protein digestion, as it represents 30%–50% of protein in plant
371 leaves and is the major dietary protein for ruminants fed forage.^{33,34} RuBisCo is a soluble
372 protein and thus readily degradable in the rumen, as solubility has been shown to be the key

373 factor determining protein susceptibility to microbial proteases. For instance, it has been
374 shown that insoluble prolamins and glutelins are slowly degraded but soluble globulins are
375 highly degradable.³⁵ Furthermore, RuBisCo is a relatively unstable protein, and disruption of
376 its quaternary structure may facilitate precipitation by tannins.^{36,37}

377 Structure of the protein, especially the presence of bonds within and between protein chains,
378 is also an important factor in rumen degradation.³⁸ Here we found a clear reduction of
379 proteolysis for both RuBisCo subunits. In contrast, condensed tannins isolated from forage
380 legumes have been shown to strongly reduce *rbcL* degradation but weakly reduce *rbcS*
381 degradation.³⁹ These differences may be due to the nature of the tannin extract tested, as we
382 used a mixture of condensed and hydrolyzable tannins, illustrating that tannin binding ability
383 varies with tannin type and source.⁴⁰

384 In the simulated abomasal compartment, the difference in proportion of soluble and
385 membrane proteins was due to a higher abundance of RuBisCo proteins after tannin infusion,
386 as demonstrated by the proteomic analysis of rumen fluid. The peptidomic analysis indicated
387 that tannin infusion leads to higher peptide release from RuBisCo and soluble proteins in
388 general, as shown by the projection of identified peptides along the protein sequence (Figure
389 3B). The higher intensity of hydrolysis for RuBisCo in the presence of tannins suggests that
390 the RuBisCo–tannin complexes could be dissociated in the physico-chemical conditions of the
391 abomasum, leading to increased peptide flow to the intestine when tannins have protected the
392 RuBisCo in the rumen. Our observations are consistent with data from literature who showed
393 that a lower pH facilitates dissociation of the condensed tannin–protein complex.⁴¹ Proteins
394 are more efficiently precipitated by tannins at pH values near their isoelectric points, and
395 protein–tannin affinity depends on the characteristics of the tannin⁴² and the size of the
396 protein: peptides with less than six residues interact weakly with tannins.⁴³ Moreover, this
397 study found a higher abundance of chloroplast stroma proteins in the tannin group, which

398 indicates that these proteins had undergone less degradation compared to the control group.
399 These proteins found in cellular fluid were likely more accessible to tannins ready to bind
400 them. Conversely, some membrane proteins were found less accessible to tannins: Gene
401 Ontology term enrichment analysis (Figure 3C) showed a higher occurrence of peptides from
402 tylakoid membrane proteins in the control group.

403 In the simulated small intestine, there was a significant decrease in the identified peptides
404 indicating that a large proportion of proteins and peptides had been digested. There was still a
405 clear between-group difference in the early stage of the intestinal digestion that was mainly
406 explained by the higher RuBisCo abundance in the tannin group. This result shows that the
407 ruminal protection conferred by tannins on RuBisCo in the rumen continues to impact
408 RuBisCo digestion at this early stage of intestinal digestion, whereas the between-group
409 difference was no longer detectable in the late stage of intestinal digestion. Taken together,
410 these results indicate that tannin intake enabled greater amounts of the main plant protein to
411 reach the small intestine where they get hydrolyzed into nutrients. This finding has important
412 implications for ruminant nutrition and environmental footprint, as it is well known that when
413 rumen-degradable proteins exceed the requirements for microbial synthesis, large amounts of
414 NH_3 get released in the rumen, absorbed into the blood, converted into urea in the liver, and
415 then excreted and volatilized into the environment via urine.⁴⁴ To optimize N use efficiency
416 by ruminants, it is necessary to minimize N intake while adequately covering energy
417 requirements for meat or milk production, thereby reducing both protein feed costs and N
418 excretion into the environment. Achieving this goal hinges on increasing the flow of
419 ruminally-synthesized microbial protein and dietary protein escaping ruminal degradation to
420 the small intestine.⁴⁵

421 In conclusion, this study found clear evidence that tannins deeply modify protein metabolism
422 in the ruminant gastrointestinal tract. In particular, RuBisCo, the main plant protein consumed

423 by forage-fed ruminants, is effectively protected by tannins against excessive degradation in
424 the rumen, and then get progressively degraded in the abomasum and small intestine. This
425 could increase the protein use efficiency by ruminants and decrease the environmental impact
426 of urinary N losses. The peptidomic approach applied here appears to be particularly well
427 suited for this kind of study, as it can help to identify and quantify the type of protein
428 hydrolyzed throughout the gastrointestinal tract in relation to tannin chemical structure. The
429 challenge remains to predict the quantitative contribution of tannin-bound protein to improve
430 N supply to the small intestine, which is an important issue as it may offer a pathway to
431 significantly decrease protein feed supplementation and thus improve protein self-sufficiency
432 for ruminant farmers.

433

434 **Abbreviations Used**

435 ADF, acid detergent fiber; CP, crude protein; DM, dry matter; DNA, deoxyribonucleic acid;
436 NDF, neutral detergent fiber; OM, organic matter; OTU, operational taxonomic unit; PCA,
437 principal component analysis; RuBisCo, ribulose biphosphate carboxylase; RuBisCo small-
438 chain (rbcs); RuBisCo large-chain (rbcl); SDS, sodium dodecyl sulfate; TCA, trichloroacetic
439 acid; VFA, volatile fatty acids.

440

441 **Acknowledgements**

442 The authors thank the staff at the ‘Herbipole’ experimental unit (INRAE Auvergne Rhône-
443 Alpes) for animal care.

444

445 **Funding sources**

446 This study received financial support from transnational funding bodies via partnership
447 agreements under the H2020 ERA-net project– CORE Organic Cofund and was cofunded by

448 the European Commission under the ProYoungStock “Promoting young stock and cow health
449 and welfare by natural feeding systems” project. The INRAE ‘Animal physiology and
450 farming’ division also provided financial support.

451

452 **Supporting information description**

453 Figure S1-S4. Shannon Simpson Evenness Richness indices and principal component (PC)
454 analysis for bacterial and protozoal communities in the rumen

455 Some supplementary data used in the development of this article (identification and
456 quantification data) were submitted in Data in Brief ([https://www.sciencedirect.com/
457 journal/data-in-brief](https://www.sciencedirect.com/journal/data-in-brief)) as a co-submission of this research article: Digestomic data of
458 proteolysis during wethers post rumen digestion after tannin supplementation, Chambon et al.
459 2021.

460

461 **References**

462 (1) United Nations. World Population Prospects 2019. URL

463 <https://population.un.org/wpp/>

464 (2) Alexandratos, N.; Bruinsma, J. In *World agriculture towards 2030/2050: the 2012*
465 *revision*, ESA working paper 12–03, Food and Agriculture Organization of the United
466 Nations, Rome, Italy, **2012**.

467 (3) Henchion, M.; Hayes, M.; Mullen, A. M.; Fenelon, M.; Tiwari, B. Future protein
468 supply and demand: strategies and factors influencing a sustainable equilibrium. *Foods* **2017**,
469 6, 53.

470 (4) Calsamiglia, S.; Ferret, A.; Reynolds, C. K.; Kristensen, N. B.; Van Vuuren, A. M.
471 Strategies for optimizing nitrogen use by ruminants. *Animal* **2010**, 4, 1184–1196.

- 472 (5) Selbie, D. R.; Buckthought, L. E.; Shepherd, M. A. The challenge of the urine patch
473 for managing nitrogen in grazed pasture systems. *Adv. Agron.* **2015**, 129, 229–292.
- 474 (6) Broucek, J. Nitrous oxide production in ruminants – A review. *Anim. Sci. Pap. Rep.*
475 **2018**, 36, 5–19.
- 476 (7) Gerber, P. J.; Steinfeld, H.; Henderson, B.; Mottet, A.; Opio, C.; Dijkman, J.; Falcucci,
477 J.; Tempio, G. *Tackling climate change through livestock: a global assessment of emissions
478 and mitigation opportunities*. Food and Agriculture Organization of the United Nations
479 (FAO), Rome, Italy; 2013.
- 480 (8) Dijkstra, J.; Reynolds, C. K.; Kebreab, E.; Bannink, A.; Ellis, J. L.; France, J.; Van
481 Vuuren, A. M. Challenges in ruminant nutrition: towards minimal nitrogen losses in cattle. In
482 *Energy and protein metabolism and nutrition in sustainable animal production*, Wageningen
483 Academic Publishers, Wageningen, The Netherland, 2013; pp. 47–58.
- 484 (9) Mueller, N. D.; Lassaletta, L. Nitrogen challenges in global livestock systems. *Nat.*
485 *Food* **2020**, 1, 400–401.
- 486 (10) Schwab, C. G.; Huhtanen, P.; Hunt, C. W.; Hvelplund, T. Nitrogen requirements of
487 cattle. In: *Nitrogen and Phosphorus Nutrition of Cattle and Environment*. CABI Publishing,
488 Wallingford, UK; 2005; pp. 13–70.
- 489 (11) Patra, A. K.; Saxena, J. Exploitation of dietary tannins to improve rumen metabolism
490 and ruminant nutrition. *J. Sci. Food Agric.* **2011**, 91, 24–37.
- 491 (12) Theron, L.; Gueugneau, M.; Coudy-Gandilhon, C.; Viala, D.; Bijlsma, A.; Butler-
492 Browne, G.; Maier, A.; Béchet, D.; Chambon, C. Label-free quantitative protein profiling of
493 vastus lateralis muscle during human aging. *Mol. Cell. Proteom.* **2014**, 13, 283–294.
- 494 (13) Ménard, O.; Cattenoz, T.; Guillemin, H.; Souchon, I.; Deglaire, A.; Dupont, D.;
495 Picque, D.. Validation of a new in vitro dynamic system to simulate infant digestion. *Food*
496 *Chem.* **2014**, 145, 1039–1045.

- 497 (14) Guillemin, H.; Perret, B.; Picque, D.; Menard, O.; Cattenoz, T.; Logiciel StoRM –
498 Stomach and duodenum Regulation and Monitoring. IDDN.FR.001.30009.000.R.P.2010.000.
499 31235, **2010**, 290.
- 500 (15) Minekus, M.; Alming, M.; Alvito, P.; Balance, S.; Bohn, T.; Bourlieu, C.; Carrière,
501 F.; Boutrou, R.; Corredig, M.; Dupont, D.; Dufour, C.; Egger, L.; Golding, M.; Karakaya, S.;
502 Kirkhus, B.; Le Feunteun, S.; Lesmes, U.; Macierzanka, A.; Mackie, A.; Marze, S.;
503 McClements, D. J.; Ménard, O.; Recio, I.; Santos, C. N.; Singh, R. P.; Vegarud, G. E.;
504 Wickham, M. S. J.; Weitschies, W.; Brodkorb, A. A standardised static *in vitro* digestion
505 method suitable for food – an international consensus. *Food Funct.* **2014**, 5, 1113–2.
- 506 (16) Elashoff, J. D.; Reedy, T. J.; Meyer, J. H. Analysis of gastric emptying data.
507 *Gastroenterology* **1982**, 83, 1306–1312.
- 508 (17) Morgavi, D. P., Martin, C.; Boudra, H. Fungal secondary metabolites from *Monascus*
509 spp. reduce rumen methane production *in vitro* and *in vivo*. *J. Anim. Sci.* **2013**, 91, 848-860.
- 510 (18) Park, G. E.; Oh, H. N.; Ahn, S. Y. Improvement of the ammonia analysis by the
511 phenate method in water and wastewater. *Bull. Korean Chem. Soc.* **2009**, 30, 2032–2038.
- 512 (19) Yu, Z.; Morrison, M. Improved extraction of PCR-quality community DNA from
513 digesta and fecal samples. *Biotechniques* **2004**, 36, 808–812.
- 514 (20) Popova, M.; Guyader, J.; Silberberg, M.; Seradj, A. R.; Saro, C.; Bernard, A.; Gérard,
515 C.; Martin, C.; Morgavi, D. P. Changes in the rumen microbiota of cows in response to
516 dietary supplementation with nitrate, linseed, and saponin alone or in combination. *Appl.*
517 *Environ. Microbiol.* **2019**, 85, e02657–18.
- 518 (21) Sayd, T.; Chambon, C.; Santé-Lhoutellier, V. Quantification of peptides released
519 during *in vitro* digestion of cooked meat. *Food Chem.* **2016**, 197, 1311–1323.

- 520 (22) Mi, H.; Muruganujan, A.; Ebert, D.; Huang, X.; Thomas, P. D. PANTHER version 14:
521 more genomes, a new PANTHER GO-slim and improvements in enrichment analysis tools.
522 *Nucleic Acids Res.* **2019**, *47*, 419–426.
- 523 (23) Binder, J. X.; Pletscher-Frankild, S.; Tsafou, K.; Stolte, C.; O'Donoghue, S. I.;
524 Schneider, R.; Jensen, L. J. COMPARTMENTS: unification and visualization of protein
525 subcellular localization evidence. *Database* **2014**, bau012.
- 526 (24) Manguy, J.; Jehl, P.; Dillon, E. T.; Davey, N. E.; Shields, D. C.; Holton, T. A.
527 Peptigram: a web-based application for peptidomics data visualization. *J. Proteome Res.*
528 **2016**, *16*, 712–719.
- 529 (25) Escudié, F.; Auer, L.; Bernard, M.; Mariadassou, M.; Cauquil, L.; Vidal, K.; Maman,
530 S.; Hernandez-Raquet, G.; Combes, S.; Pascal, G. FROGS: find, rapidly, OTUs with galaxy
531 solution. *Bioinformatics* **2018**, *34*, 1287–1294.
- 532 (26) Oskansen, J.; Blanchet, F.; Kindt, R. vegan: community ecology package. R package
533 version 2.0-7. URL <https://cran.r-project.org/web/packages/vegan/index.html>; **2016**.
- 534 (27) Hervás, G.; Pérez, V.; Giráldez, F. J.; Mantecón, A. R.; Almar, M. M.; Frutos, P.
535 Intoxication of sheep with quebracho tannin extract. *J. Comp. Pathol.* **2003**, *129*, 44–54.
- 536 (28) Allison M., J. Production of branched-chain volatile fatty acids by certain anaerobic
537 bacteria. *Appl. Environ. Microbiol.* **1978**, *35*, 872–877.
- 538 (29) Abdoun, K.; Stumpff, F.; Martens, H. Ammonia and urea transport across the rumen
539 epithelium: a review. *Anim. Health Res. Rev.* **2006**, *7*, 43–59.
- 540 (30) Bannink, A.; Kogut, J.; Dijkstra, J.; France, J.; Kebreab, E.; Van Vuuren, A. M.;
541 Tamminga, S. Estimation of the stoichiometry of volatile fatty acid production in the rumen
542 of lactating cows. *J. Theor. Biol.* **2006**, *238*, 36–51.

- 543 (31) Min, B. R.; Solaiman, S. Comparative aspects of plant tannins on digestive
544 physiology, nutrition and microbial community changes in sheep and goats: a review. *J. Anim.*
545 *Physiol. Anim. Nutr.* **2018**, 102, 1181–1193.
- 546 (32) Diaz Carrasco, J. M.; Cabral, C.; Redondo, L. M.; Pin Viso, N. D.; Colombatto, D.;
547 Farber, M. D.; Fernandez Miyakawa, M. E. Impact of chestnut and quebracho tannins on
548 rumen microbiota of bovines. *Biomed Res. Int.* **2017**, 1–11.
- 549 (33) McNabb, W. C.; Peters, J. S.; Foo, L. Y.; Waghorn, G. C.; Jackson, F. C. Effect of
550 condensed tannins prepared from several forages on the *in vitro* precipitation of ribulose-1,
551 5-bisphosphate carboxylase (Rubisco) protein and its digestion by trypsin (EC 2.4. 21.4) and
552 chymotrypsin (EC 2.4. 21.1). *J. Sci. Food Agric.* **1998**, 77, 201–212.
- 553 (34) Andersson, I.; Backlund, A. Structure and function of Rubisco. *Plant Physiol.*
554 *Biochem.* **2008**, 46, 275–291.
- 555 (35) Romagnolo, D.; Polan, C. E.; Barbeau, W. E. Electrophoretic analysis of ruminal
556 degradability of corn proteins. *J. Dairy Sci.* **1994**, 77, 1093–1099.
- 557 (36) Dobрева, M. A.; Frazier, R. A.; Mueller-Harvey, I.; Clifton, L. A.; Gea, A.; Green, R.
558 J. Binding of pentagalloyl glucose to two globular proteins occurs via multiple surface sites.
559 *Biomacromolecules* **2011**, 12, 710–715.
- 560 (37) Zeller, W. E.; Sullivan, M. L.; Mueller-Harvey, I.; Grabber, J. H.; Ramsay, A.; Drake,
561 C.; Brown, R. H. Protein precipitation behavior of condensed tannins from *Lotus*
562 *pedunculatus* and *Trifolium repens* with different mean degrees of polymerization. *J. Agric.*
563 *Food Chem.* **2015**, 63, 1160–1168.
- 564 (38) Bach, A.; Calsamiglia, S.; Stern, M. D. Nitrogen metabolism in the rumen. *J. Dairy*
565 *Sci.* **2005**, 88, E9-E21.
- 566 (39) Tanner, G. J.; Moore, A. E.; Larkin, P. J. Proanthocyanidins inhibit hydrolysis of leaf
567 proteins by rumen microflora *in vitro*. *Br. J. Nutr.* **1994**, 71, 947–958.

- 568 (40) Engström, M. T.; Arvola, J.; Nenonen, S.; Virtanen, V. T.; Leppä, M. M.; Tähtinen,
569 P.; Salminen, J. P. Structural features of hydrolyzable tannins determine their ability to form
570 insoluble complexes with bovine serum albumin. *J. Agric. Food Chem.* **2019**, *67*, 6798–6808.
- 571 (41) Jones, W. T.; Mangan, J. L. Complexes of the condensed tannins of sainfoin
572 (*Onobrychis viciifolia* Scop.) with fraction 1 leaf protein and with submaxillary mucoprotein,
573 and their reversal by polyethylene glycol and pH. *J. Sci. Food Agric.* **1977**, *28*, 126–136.
- 574 (42) Mueller-Harvey, I.; Bee, G.; Dohme-Meier, F.; Hoste, H.; Karonen, M.; Kolliker, R.;
575 Lüscher, A.; Niderkorn, V.; Pellikaan, W. F.; Salminen, J. P.; Skot, L.; Smith, L. M. J.;
576 Thamsborg, S. M.; Totterdell, P.; Wilkinson, I.; Williams, A. R.; Azuhwi, B. N.; Baert, N.;
577 Grosse Brinkhaus, A.; Copani, G.; Desrues, O.; Drake, C.; Engstrom, M.; Fryganas, C.;
578 Girard, M.; Huyen, N. T.; Kempf, K.; Malisch, C.; Mora-Ortiz, M.; Quijada, J.; Ramsay, A.;
579 Ropiak H. M.; Waghorn, G. C. Benefits of condensed tannins in forage legumes fed to
580 ruminants: importance of structure, concentration and diet composition. *Crop Sci.* **2019**, *59*,
581 861–885.
- 582 (43) Hagerman, A. E.; Butler, L. G. The specificity of proanthocyanidin–protein
583 interactions. *J. Biol. Chem.* **1981**, *256*, 4494–4497.
- 584 (44) Muck, R. E. Urease activity in bovine feces. *J. Dairy Sci.* **1982**, *65*, 2157–2163.
- 585 (45) Tomlinson, D. L.; James, R. E.; Bethard, G. L.; McGilliard, M. L. Influence of
586 undegradability of protein in the diet on intake, daily gain, feed efficiency, and body
587 composition of Holstein heifers. *J. Dairy Sci.* **1997**, *80*, 943–948.

588

589 Captions

590 **Figure 1.** *In vitro* abomasal-intestinal dynamic digestion

591 **Legend:** (A) Schematic representation of the ovine digestive tract. (B) Implementation of
592 infused rumen and *in vitro* dynamic digestion system DiDGI® constituted by three

593 compartments: abomasum, duodenum / jejunum, and ileum. The last two mimic the intestinal
594 digestion. (C) *In vitro* dynamic digestion parameters in abomasum and small intestine
595 compartments: fasted volume ^{a,15}, pH, secretions, transit time ^{b,16}, and sampling time-points.
596 SGI: Simulated gastric fluid; SIF: simulated intestinal fluid.

597

598 **Figure 2.** Comparative proteomic analysis of rumen fluid from wethers infused with a tannin
599 extract (n=3) or with water (n=3).

600 **Legend:** (A) Principal component analysis of ‘Tannin’ (in red) and ‘Control’ (in blue) protein
601 abundances. On the left, the score plot shows sample projections according to the first two
602 principal components (PC1 and PC2), and the respective confidence ellipses are indicated. On
603 the right, the loading plot of the first two principal components indicates the variable
604 contribution to PC1 and PC2. The proteins are represented by their gene name, and the most
605 notable contribution from RuBisCo small (rbcS gene) and large (rbcL gene) chains is
606 indicated by a circle. (B) Quantitation of RuBisCo small (rbcS gene) and large (rbcL gene)
607 chains in rumen infused with a tannin extract (Tannin, in red) or with water (Control, in blue);
608 **p* < 0.05. (C) Representation in 3D of the isotopic pattern and abundance of the most intense
609 peptide TFQGPPHGIQVER identified from RuBisCo small chain (rbcS) on the left and
610 LPLFGATDSSQVLKELADCK identified from RuBisCo large chain (rbcL).

611

612 **Figure 3.** Comparative peptidomic analysis of *in vitro* digestion in simulated abomasum of
613 rumen fluids from wethers infused with a tannin extract (n=3) or with water (n=3).

614 **Legend:** (A) Principal component analysis of ‘Tannin’ (T, in red) and ‘Control’ (C, in blue)
615 protein abundances based on the summed abundances of the peptides resulting from their
616 abomasal digestion. The score plot shows the samples projection according to the first two
617 principal components (PC1 and PC2). The different incubation points, after 15 (A15) and 60

618 (A60) minutes of abomasal digestion, and the respective confidence ellipses are indicated. (B)
619 The loading plot of the first principal component indicates the variable contribution to PC1 as
620 a circle, blue and red shades for negative and positive contribution, respectively. The proteins
621 are represented by their gene name. (C) Statistical terms enrichment analysis using Panther
622 tools²² and Gene Ontology (GO) cellular compartment information, represented at the cellular
623 scale using the Compartment tool.²³ The proteins involved in the cellular compartment
624 resulting from enrichment analysis are indicated in bold.

625

626 **Figure 4.** Comparative peptidomic analysis of *in vitro* digestion in intestine of samples from
627 rumen fluids from wethers infused with a tannin extract (n=3) or with water (n=3).

628 **Legend:** (A) Principal component analysis of ‘Tannin’ (T, in red) and ‘Control’ (C, in blue)
629 protein abundances based on the summed abundances of the peptides resulting from their
630 intestinal digestion. The score plot shows the samples projection according to the first two
631 principal components (PC1 and PC2). The different kinetic point, after 60 (I60) and 180
632 (I180) minutes of intestinal digestion, and the respective confidence ellipses are indicated. (B)
633 Visualization of peptides released during abomasal and intestinal digestion using Peptigram.²⁴
634 The peptides resulting from the RuBisCo large chain (*rbcL* gene), and one protein from the
635 photosystems I (*psaB* gene) digestion are plotted according to the digestion kinetic: after 15
636 (A15) and 60 (A60) minutes of abomasal digestion and after 60 (I60) and 180 (I180) minutes
637 of intestinal digestion in Tannins and Control samples. Each line is a sample and for each
638 residue (on the *x* axis), a green bar is drawn along the protein sequence, if this position is
639 covered by at least one peptide in the given sample. The height of this bar is proportional to
640 the count of peptides overlapping this position and the colour intensity is proportional to the
641 summed ion intensities of peptides overlapping this position.

642

643 Table 1. Rumen fermentation end-products (volatile fatty acids (VFA) and ammonia (NH₃))
 644 in wethers fed with alfalfa and ruminally infused with a tannin extract (Tannin, n =3) or with
 645 water (Control, n = 3)

	Control	Tannin	SEM	<i>p</i> -value
<i>Fermentation end-products (mmol/l)</i>				
Total VFA	137.0	123.0	3.95	< 0.001
Acetate	101.2	90.2	2.61	< 0.001
Propionate	20.0	18.6	1.19	0.061
Butyrate	9.35	9.40	0.96	0.961
Valerate	0.96	1.05	0.123	0.240
Caproate	0.13	0.05	0.022	< 0.001
Acetate:propionate ratio	4.53	5.11	0.235	0.070
Iso-butyrate	2.32	1.47	0.105	< 0.001
Iso-valerate	3.07	2.32	0.189	< 0.001
Total iso-VFA	5.38	3.79	0.284	< 0.001
NH ₃	16.8	12.1	1.06	< 0.001

646